Original Research Article

Contribution of the Provençal well for the improvement of the thermal comfort in the building in turbulent regime

ABSTRACT

In the current energy context, geothermal systems are highly developed in the building field. Among these interesting systems on the energy plan, one finds in particular the air-soil exchangers commonly called 'Canadian or Provençal well'. It consists of tubes buried in which the ambient air is pushed in order to be refreshed in contact with the ground whose temperature is quasi-constant throughout the year. In this work, a study of the performance of an air-to-ground heat exchanger was undertaken by means of numerical modeling of heat exchange by forced convection in a buried tube. The transfer equations in the tube are discretized using the finite volume method in turbulent regime and solved using the Thomas algorithm. For the determination of the ground temperature, the model of the semi-infinite mass subjected to a periodic excitation was adopted. The evaluation of this temperature was used as a boundary condition for the buried tube.

The results show that the interest of the air-to-ground heat exchanger is major, since it improves throughout the year, the thermal conditions sought. It intervenes in an effective way on the damping of the thermal amplitudes in the building. The influence of some parameters, namely: the depth, the diameter and the length of the tube on the interior temperature of the exchanger were analyzed. The results show that the interest of the air-to-ground heat exchanger is major, since it improves throughout the year, the thermal conditions sought. It intervenes in an effective way on the damping of the thermal amplitudes in the building. The influence of some parameters, namely: the depth, the diameter and the length of the tube on the interior temperature of the exchanger were analyzed.

Keywords: *Air to ground heat exchanger - Canadian well - Geothermal energy - Building air conditioning.*

1. INTRODUCTION

In this work, the thermal performance of an air/ground heat exchanger is studied under Togo meteorological conditions for turbulent air flow in the pipeline. A mathematical model based on the conservation equations of momentum, heat to which we associated a k-ε closure model. The ground temperature is determined analytically and used as boundary conditions for the exchanger. The set of equations and boundary conditions were discretized using the finite volume method and solved by the THOMA algorithm. The results are presented in the form of streamlines and isotherms. The influence of the operating parameters (diameter, length, Reynolds number) on the distribution of the temperature and velocity fields has been studied. Forced convection in pipes is important in many applications in building heating and

especially in heat exchangers. Considerable work has been done in recent years on flows and heat transfers in air-ground heat exchangers. Such works are of particular interest in the heating and cooling of premises. These studies are both experimental [1], [2] and [3] and numerical [4]. They essentially show that the temperature at the exchanger outlet is decreased in summer and increased in winter, the friction coefficient increases with the Reynolds number. Turbulence models have also been the subject of numerous studies. One can distinguish the work of [5] who proposed, for the first time, a low Reynolds number (LRN) k-ε model by presenting attenuation functions based on the turbulent Reynolds number. In this work, the thermal behavior of a turbulent air flow under forced convection in a U-shaped channel is numerically studied. This study can be a real application in the field of air-ground heat exchangers. As energy conservation is becoming more and more necessary, ground temperature data is an important aspect of the calculation of energy requirements, e.g. to determine heat losses in basements as well as to examine the possibility of using the ground as a source for geothermal systems, i.e. heat pumps, bioclimatic wells etc [6-8].

2. PROBLEM FORMULATION

2.1. Problem configuration and assumptions

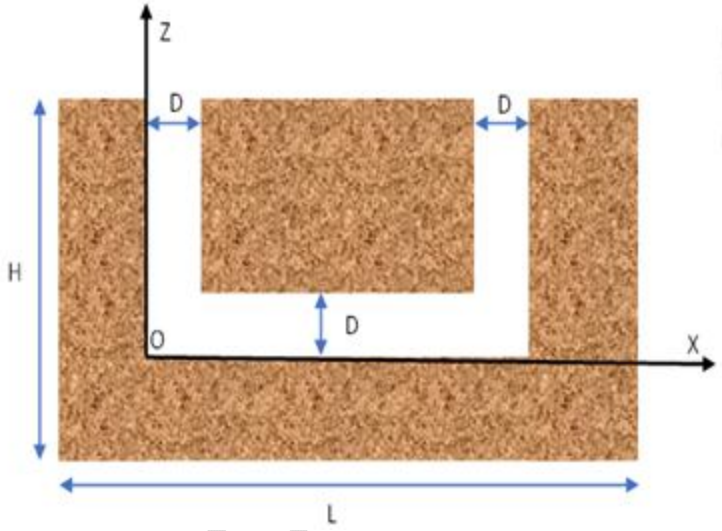

Figure 1 : Diagram of the physical model of the turbulence

The geometry of the considered problem is a buried pipe at a depth H in which the air flows. This duct has a length L and an internal diameter D. The air enters the duct through the left opening with an ambient temperature Ta and a velocity U0. The geometry of the system is shown in the

To facilitate the reading of the figure1, we will designate by compartment 1, the left vertical part of the exchanger where the air enters, compartment 2, the horizontal part of the exchanger and compartment 3, the right vertical part leading to the exchanger outlet or to the building.

2.2. Heat transfer equation in soil

In the study of the air/ground exchanger we will consider the soil as a semi-infinite medium. In this condition, the heat equation is written:

$$\frac{\partial T_{sol}}{\partial t} = \alpha_{sol} \frac{\partial^2 T_{sol}}{\partial z^2} \#(1)$$

With :

$$T_{sol}(0,t) = T_0 + A_T Cos\,[\omega(t - t_0)]\#(2)$$

$T_{sol}(\infty,t) = T_0$ (3)

où $T_0 = \frac{T_{min}+T_{max}}{2}$ et $A_T = \frac{T_{max}-T_{min}}{2}$ (4)

The analytical solution of this equation gives:

$$T_{Sol}(x,t) = T_0 + A_T exp\left(-x\sqrt{\frac{\omega}{2\alpha_{sol}}}\right).cos\left(\omega(t - t_0) - x\sqrt{\frac{\omega}{2\alpha_{sol}}}\right) \quad (5)$$

2.3. Transfer equation within the heat exchanger

The study of fluid flow cannot be approached without first establishing a number of simplifying hypotheses. In this study, we will assume that:
The flow is unsteady and turbulent.
Flow is considered two-dimensional.
The fluid is supposed Newtonian, and incompressible.
There are no heat sources in the exchanger.
Radiant heat transfer is negligible.
Heat dissipation by viscous friction is neglected.
The Boussinesq approximation is considered.
The basic equations governing heat flow and transfer are given as follows: :

2.4 Turbulence model

There are different turbulence models which differ in their degree of complexity, i.e. in the number of additional transport equations introduced to evaluate the turbulent quantities (closure equations). In this work we used the low Reynolds number model of Launder and Sharma [9] [10] introduced in 1974. We have chosen this model because it does not depend explicitly on the distance to the wall, which makes it very flexible. According to this model, the dimensional form of the turbulent kinetic energy equation and the equation of its dissipation function are expressed by the following relations:
Continuity equation

$$\frac{\partial u}{\partial x} + \frac{\partial v}{\partial y} = 0 \quad (6)$$

Equation for conserving the following momentum (ox)

$$\frac{\partial u}{\partial t} + \frac{\partial}{\partial x}(uu) + \frac{\partial}{\partial y}(vu) = -\frac{1}{\rho_0}\frac{\partial}{\partial x}\left(p + \frac{2}{3}\rho_0 k\right) + \frac{\partial}{\partial x}\left[2(\nu + \nu_t)\left(\frac{\partial u}{\partial x}\right)\right] + \frac{\partial}{\partial y}\left[(\nu + \nu_t)\left(\frac{\partial u}{\partial y} + \frac{\partial v}{\partial x}\right)\right] \quad (7)$$

Equation for conservation of the following momentum (oy)

$$\frac{\partial v}{\partial t} + \frac{\partial}{\partial x}(uv) + \frac{\partial}{\partial y}(vv) = -\frac{1}{\rho_0}\frac{\partial}{\partial y}\left(p + \frac{2}{3}\rho_0 k\right) + \frac{\partial}{\partial x}\left[(\nu + \nu_t)\left(\frac{\partial u}{\partial y} + \frac{\partial v}{\partial x}\right)\right] + \frac{\partial}{\partial y}\left[2(\nu + \nu_t)\left(\frac{\partial v}{\partial x}\right)\right] + \rho g\beta\left(\theta - \theta_0\right) \quad (8)$$

Energy conservation equation

$$\frac{\partial \theta}{\partial t} + \frac{\partial}{\partial x}(u\theta) + \frac{\partial}{\partial y}(v\theta) = \frac{\partial}{\partial x}\left[\left(\frac{\nu}{Pr\frac{\nu_t}{\sigma_t}}\frac{\partial \theta}{\partial x}\right)\right] + \frac{\partial}{\partial y}\left[\left(\frac{\nu}{Pr\frac{\nu_t}{\sigma_t}}\frac{\partial \theta}{\partial y}\right)\right] \quad (9)$$

$$Turbulent\ kinetic\ energy\ equation$$

$$\frac{\partial k}{\partial t} + \frac{\partial}{\partial x}(uk) + \frac{\partial}{\partial y}(vk) = \frac{\partial}{\partial x}\left[\left(\nu + \frac{\nu_t}{\sigma_k}\right)\frac{\partial k}{\partial x}\right] + \frac{\partial}{\partial y}\left[\left(\nu + \frac{\nu_t}{\sigma_k}\right)\frac{\partial k}{\partial y}\right] +$$

(10)

$$P_k + G_k - \varepsilon^* - D$$

Turbulent kinetic energy dissipation rate equation

$$\frac{\partial \varepsilon^*}{\partial t} + \frac{\partial}{\partial x}(u\varepsilon^*) + \frac{\partial}{\partial y}(v\varepsilon^*) = \frac{\partial}{\partial x}\left[\left(\nu + \frac{\nu_t}{\sigma_\varepsilon}\right)\frac{\partial \varepsilon^*}{\partial x}\right] + \frac{\partial}{\partial y}\left[\left(\nu + \frac{\nu_t}{\sigma_\varepsilon}\right)\frac{\partial \varepsilon^*}{\partial y}\right]$$

$$+C_1 f_1 \frac{\varepsilon^*}{k}\left(P_k + C_3 G_k\right) - C_2 f_2 \frac{\varepsilon^{*2}}{k} + E$$

(11)

$$\text{Avec :} \begin{cases} P_k = 2\nu_t\left[\left(\frac{\partial u}{\partial x}\right)+\left(\frac{\partial v}{\partial y}\right)\right] + \nu_t\left[\left(\frac{\partial v}{\partial x}\right)+\left(\frac{\partial u}{\partial y}\right)\right] \\ G_k = -g\beta\frac{\nu_t}{\sigma_t}\left(\frac{\partial \theta}{\partial y}\right) \\ D = 2\nu\left[\left(\frac{\partial \sqrt{k}}{\partial x}\right)^2 + \left(\frac{\partial \sqrt{k}}{\partial y}\right)^2\right] \\ E = 2\nu\nu_t\left[\left(\frac{\partial^2 u}{\partial y^2}\right)+\left(\frac{\partial^2 v}{\partial x^2}\right)\right] \end{cases} \quad (12)$$

$$\nu_t = C_\mu f_\mu \frac{k^2}{\varepsilon} \; ; \quad f_\mu = exp\left(\frac{-3.4}{\left(1+\frac{Re_T{}^2}{50}\right)^2}\right) \; ; \quad f_1 = 1 \; ; \quad f_2 = 1 - 0.3\,exp\left(-Re_T{}^2\right)$$

(13)

The constants of the model are:

C_μ	σ_t	σ_k	σ_ϵ	C_1	C_2	C_3
0.09	1	1	1.3	1.44	1.92	0.70

2.5. Initial and limits conditions

2.5.1. Initial conditions

The initial conditions used to resolve the issue are as follows:

A t = 0, $u = 0$; $v = 0$; $T = T_0$; $k = 10^{-3}$; $\varepsilon^* = 10^{-3}$ (14)

2.5.2. Limits conditions

To solve the equations that govern the phenomenon studied, we associated the following boundary conditions:

At the entrance of the interchange: $0 \leq x \leq D$, $y = H$

$u = 0$; $= -V_0$; $T = T_0$; $k_e = 0{,}005v_0^2$, $\varepsilon = 0{,}01k_e^2$; $P = P_0$ (15)

At the exit of the interchange: $L - D \leq x \leq L$, $y = H$

$\left.\frac{\partial u}{\partial y}\right|_{y=H} = 0$; $\left.\frac{\partial v}{\partial y}\right|_{y=H} = 0$; $\left.\frac{\partial T}{\partial y}\right|_{y=H} = 0$; $\left.\frac{\partial k}{\partial y}\right|_{y=H} = 0$; $\left.\frac{\partial \varepsilon}{\partial y}\right|_{y=H} = 0$; $\left.\frac{\partial P}{\partial y}\right|_{y=H} = 0$ (16)

Left vertical sides of compartment 1: $x = 0$; $0 \leq y \leq H$

$u = v = 0$; $= T_{sol}$; $k = 0$; $\varepsilon^* = 0$; $\left.\frac{\partial P}{\partial x}\right|_{x=0} = 0$ (17)

Right vertical sides of compartment 1: $x = D$; $D \leq y \leq H$

$u = v = 0$; $= T_{sol}$; $k = 0$; $\varepsilon^* = 0$; $\left.\frac{\partial P}{\partial x}\right|_{x=D} = 0$ (18)

Lower horizontal sides of compartment 2 : $0 \leq x \leq L$, $y = 0$

$u = v = 0$; $= T_{sol}$; $k = 0$; $\varepsilon^* = 0$; $\left.\frac{\partial P}{\partial y}\right|_{y=0} = 0$ (19)

Upper horizontal sides of the compartment 2 : $D \leq x \leq L - D$, $y = D$

$u = v = 0$; $= T_{sol}$; $k = 0$; $\varepsilon^* = 0$; $\left.\frac{\partial P}{\partial y}\right|_{y=D} = 0$ (20)

Left vertical sides of compartment 3 : $x = L - D$; $D \leq y \leq H$

$u = v = 0$; $= T_{sol}$; $k = 0$; $\varepsilon^* = 0$; $\left.\frac{\partial P}{\partial x}\right|_{x=L-D} = 0$ (21)

Right vertical sides of compartment 3: $x = L$; $0 \leq y \leq H$

$u = v = 0$; $= T_{sol}$; $k = 0$; $\varepsilon^* = 0$; $\left.\frac{\partial P}{\partial x}\right|_{x=L} = 0$ (22)

2.6. Discretization of equations

2.6.1. Transport equation

The general transport equation of a variable evolving in a two-dimensional incompressible flow is written in the Cartesian system as follows:

$$\frac{\partial \phi}{\partial \tau} + \frac{\partial}{\partial X_j}\left(U_j \phi\right) = \frac{\partial}{\partial X_j}\left(\Gamma \frac{\partial \phi}{\partial X_j}\right) + S_\phi \quad (23)$$

With $j \epsilon \{1; 2\}$ (index of summation)

$\frac{\partial \phi}{\partial \tau}$: Transient term that represents the accumulation of Φ over time.

$\frac{\partial}{\partial X_j}\left(U_j \phi\right)$: transport of Φ by convection, $\frac{\partial}{\partial X_j}\left(\Gamma \frac{\partial \phi}{\partial X_j}\right)$: diffusion transport of Φ, Γ : diffusion coefficient, S_φ: source term.

The general form of the discretized algebraic equation is as follows: :

$a_P \phi_P = a_E \phi_E + a_W \phi_W + a_N \phi_N + a_S \phi_S + b$ (24)

The source term is discretized using a finite difference method and then linearized as a function of variable ϕ at node P.

$\overline{S} = S_c + S_P \phi_P$

For the numerical solution of the equations of this thesis we have opted for the TDMA method. With this method the algebraic equations obtained previously can be written in the following general form:

$A(I,J)\phi(I,J-1) + B(I,J)\phi(I,J) + C(I,J)\phi(I,J+1) = D(J)$ (25)

The resulting system of algebraic equations is a tridiagonal system of algebraic equations solved using the Thomas algorithm [11] associated with an iterative procedure with a sub-relaxation coefficient equal to 0.5 for the velocity components and 0.8 for the temperature, turbulent kinetic energy, energy dissipation rate and pressure.
In order to satisfy the principle of conservation of mass and energy at each time step, the following convergence criterion must be verified for each variable :

$$\frac{Max\left(|\phi(I,J)^{k+1}-\phi(I,J)^{k}|\right)}{|\phi^{k}(I,J)|} \leq \epsilon \qquad (26)$$

Where k represents the number of iterations and ϵ the precision taken at 10^{-4}.

2.6.2. Validation of numerical code

To validate our calculation code, the numerical results obtained are compared with the experimental results obtained by F. Ampofo et al [12] and the numerical results of Henkes et al [13]. The present validation was obtained in fortran90 language. The 180 X 180 mesh with mesh refinement was performed. The k-epsilon model is used. The calculation was performed on a real time of 500 seconds.

Temperature profile comparison at y = 0.5

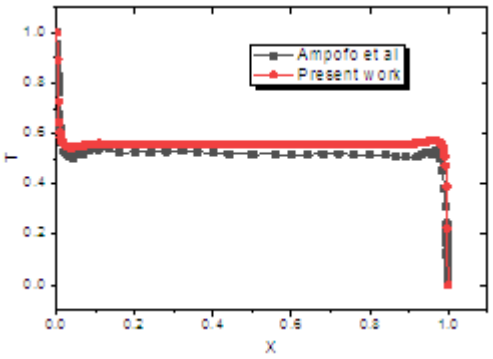

Comparison of velocity profiles at y = 0.5

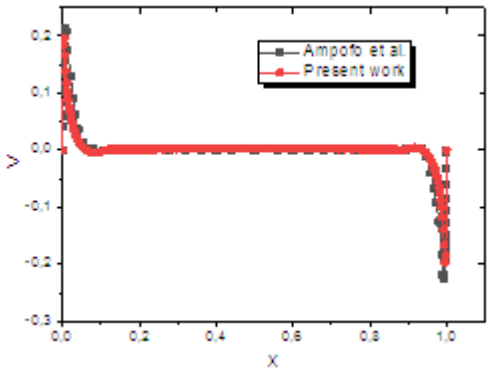

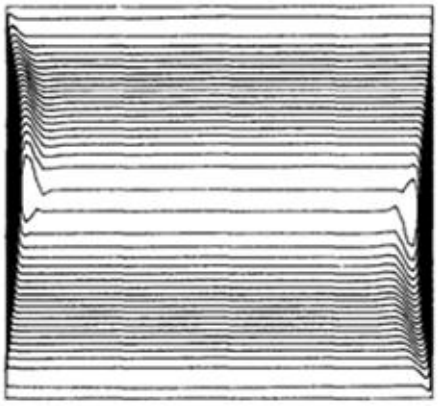

Model of Henkes et al

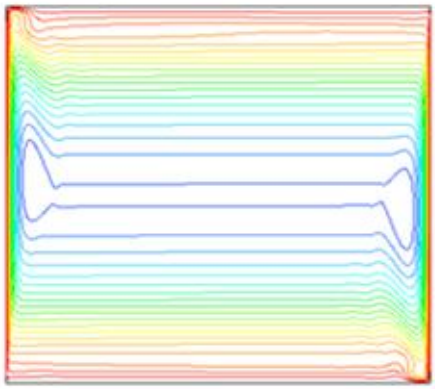

Our model comparison of power lines

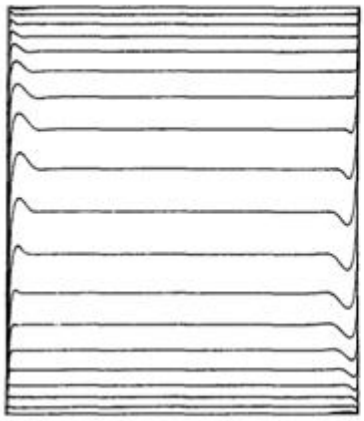

Model of Henkes et al

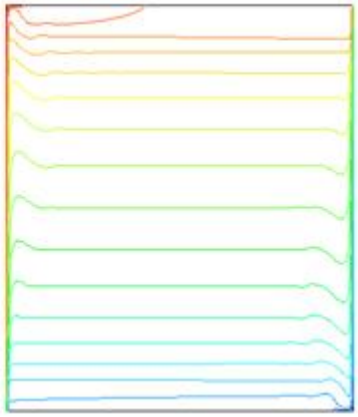

Our model

Comparison of isotherms

Model of Henkes et al

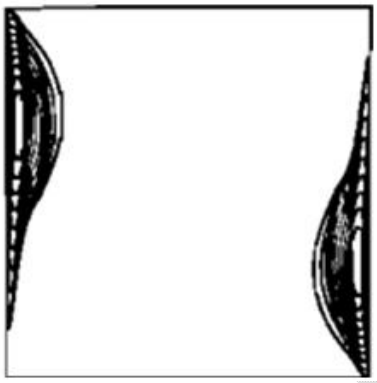

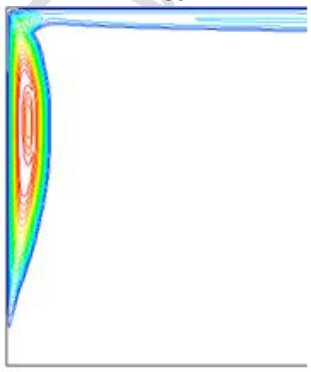

Our model

Comparison of the isovals of the turbulent viscosity

Image 1 : k-epsilon model

2.6.3. Study of the influence of the operating parameters of the air/soil exchanger
2.6.3.1. Influence of the diameter
2.6.3.2. Flow structure

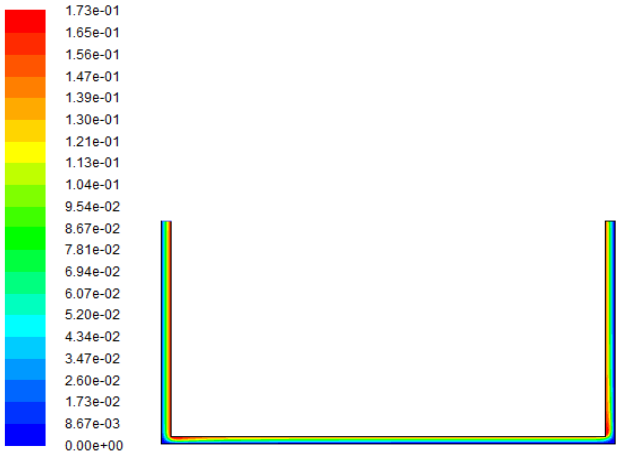

D=0,2 m

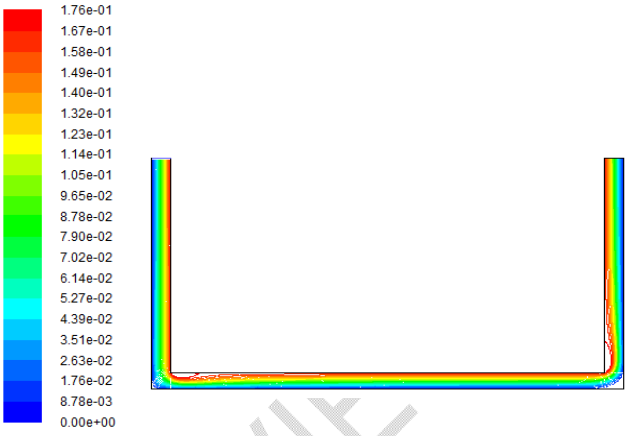

D=0,4 m

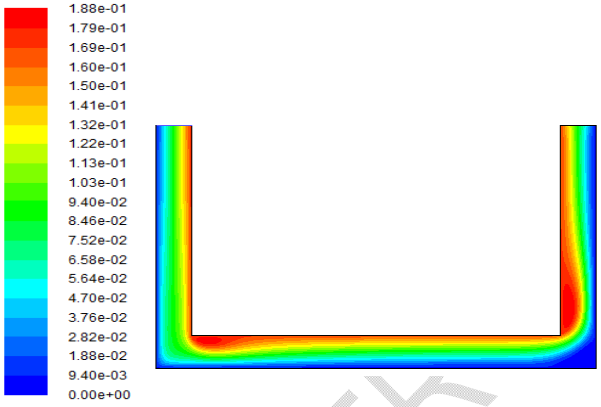

D=0,8 m

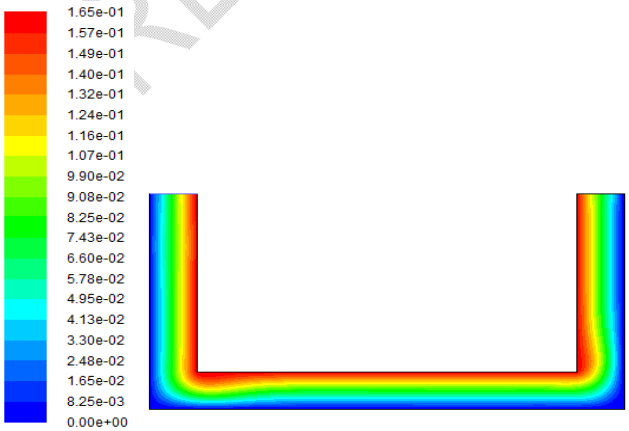

D=1,0 m

Figure 2: Distribution of current lines for Re=400 for different diameters

Figure 2 shows the influence of the duct diameter on the flow. It can be seen that for a small duct diameter (0.2 m), the flow structure over the entire duct is illegible. We have chosen different values of the diameter: 0.4 ; 0.8 et 1.0 m. It can be seen that the variation of the diameter does not significantly influence the structure of the current lines. However, an increase in the values of the current function is noted as the diameter increases. But for a larger diameter (D=1 m), a decrease of the streamlines was observed. This shows that the choice of the diameter can influence the intensity of the forced convection in the channel.

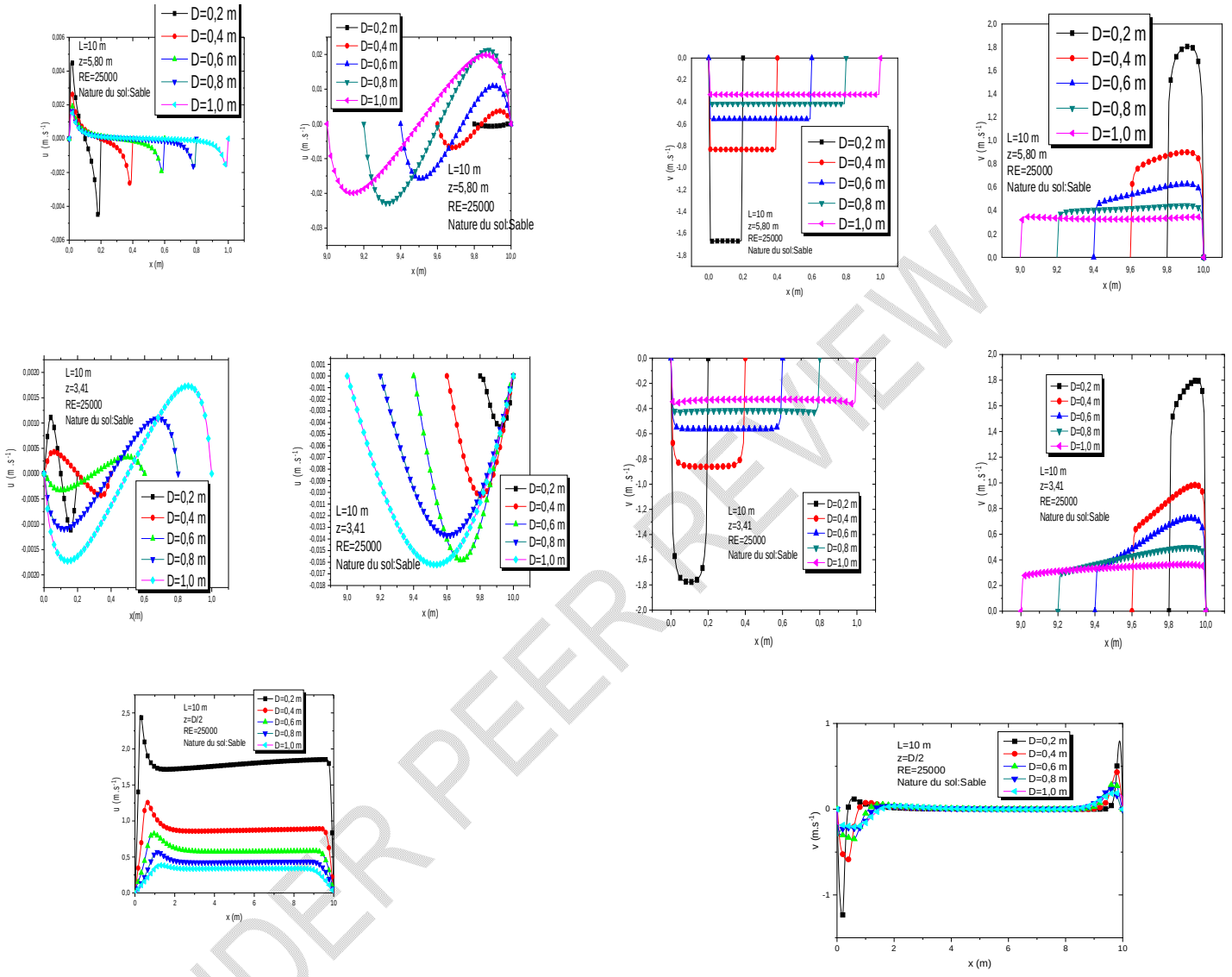

Figure 3 : Profile of the u and v components of the velocity under the influence of the diameter of the exchanger

Figure 3 shows the profile of the horizontal component of the velocity as a function of x for different values of the diameter in several sections of the exchanger. It can be seen that the variation of the diameter has a considerable influence on the shape of the velocities in the different compartments of the exchanger. Near the inlet the profiles of the horizontal component of the velocity (u) are similar for different values of the diameter. But the values of the amplitudes of u decrease when the diameter increases. In compartment 3, the variation of the diameter shows that the velocity profile is not changed when varying the diameter in each section of the compartment. However, from one section to another, a difference in the u profiles can be observed. The analysis of the figures in compartments 2 and 3 reveals that the values of the amplitude of the horizontal component of the velocity

increase with the diameter. The change in sign of the u component of the velocity observed in compartments 1 and 3 shows that the fluid sometimes flows towards the left or right side of compartment 1 and 3.

Contrary to the horizontal component of the velocity, we note that the vertical component of the velocity keeps the same shape and sign in the vertical parts of the exchanger. In compartment 1, the negative sign of v indicates that the flow is from top to bottom, while in compartment 3, the positive sign means that the air flow is from bottom to top. It can also be seen that the amplitude of the component decreases as the diameter increases.

2.6.3.3. Temperature field

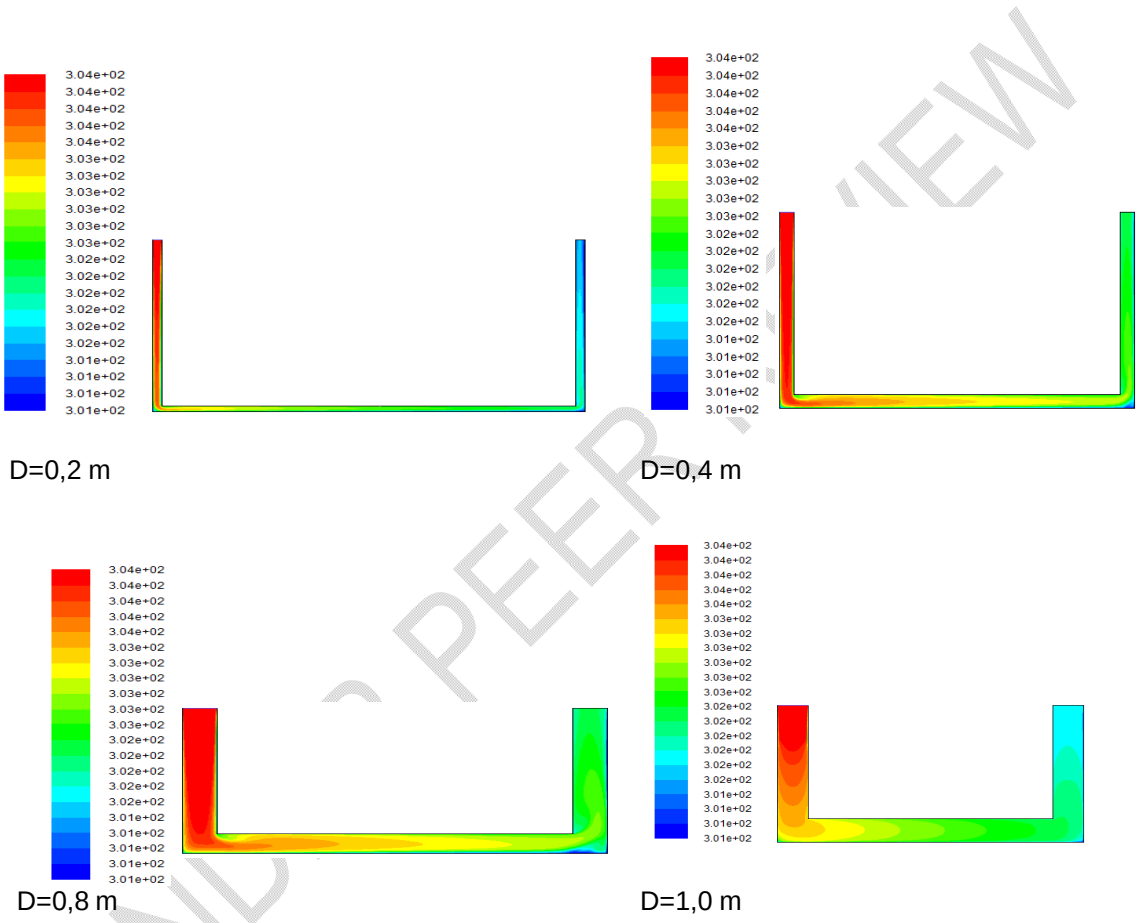

Figure 4: Distribution of isotherms under the influence of the diameter of the exchanger

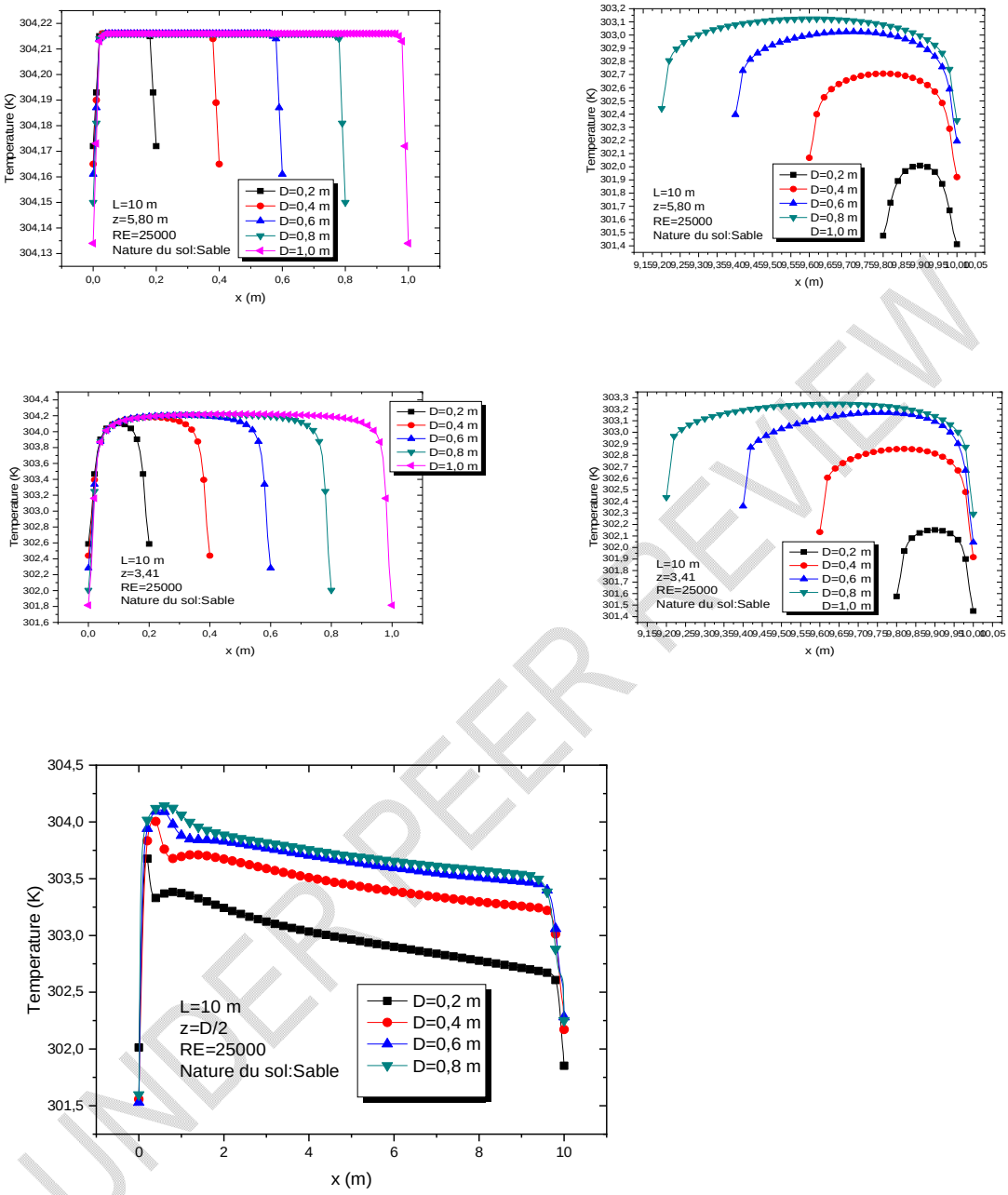

Figure 5: Temperature profile under the influence of exchanger diameter

Figure 4 shows the distribution of isotherms in the "U" shaped air/soil exchanger for different values of the diameters. An analysis of this figure showed that the isotherm distributions are similar for the different diameters considered. However, the thermal field increases as the diameter increases. The minimum and maximum values of the temperatures remain identical whatever the diameter.

The analysis of the profiles shows that the temperatures keep the same pattern for the different diameters. In the air inlet compartment the temperature amplitudes in one section are the same when the diameter varies. For the horizontal part of the exchanger and in the outlet compartment the temperatures have the same trend for all diameters. However, the temperature amplitude increases when the diameter increases. Indeed, the diameter of the pipe defines the total section through which the air will circulate. It influences both the air flow speed and the contact surface between the air and the ground. As the diameter of the pipe increases, the outlet temperature increases resulting in a reduction of the heat transfer coefficient at the inner surface of the pipe. As a result, the cooling potential of the air/ground heat exchanger decreases as the diameter increases.

2.6.3.4. Temperature fields

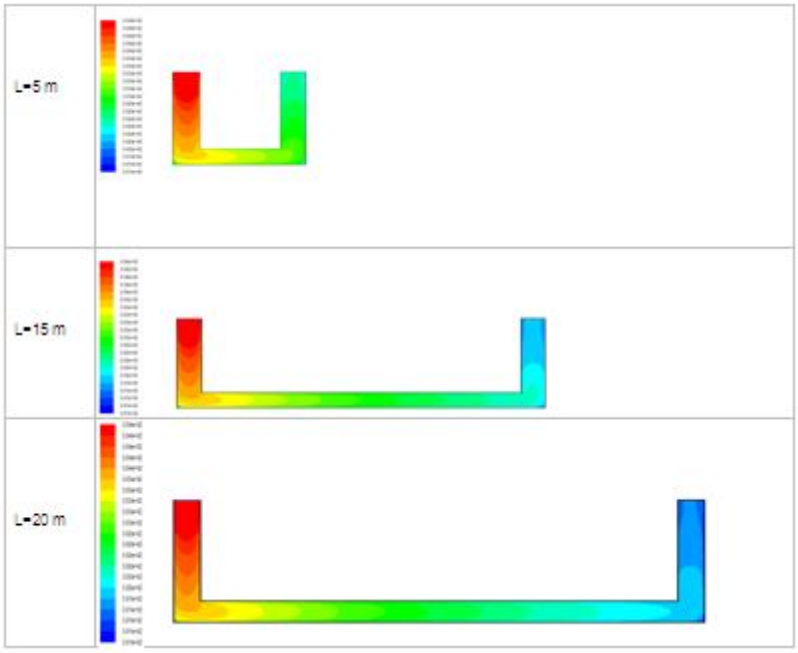

Figure 6 : Distribution of isotherms for different lengths

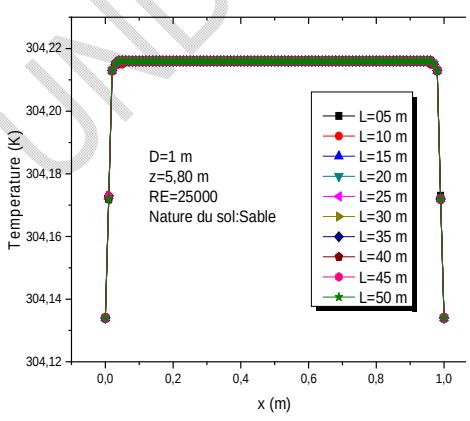

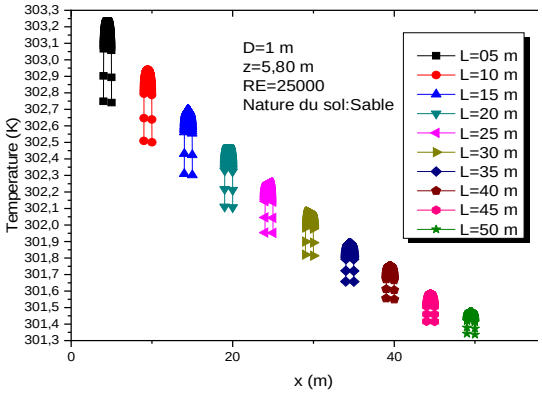

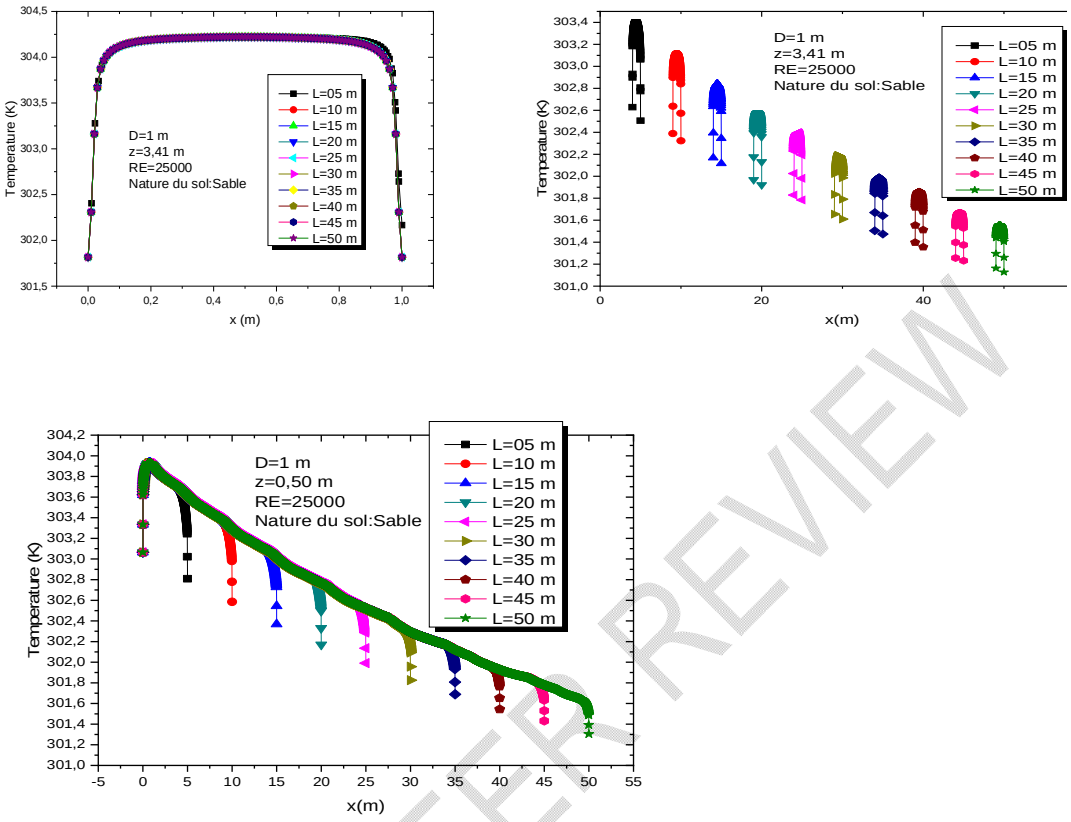

Figure 7: Temperature profile under the influence of the exchanger length

The thermal field (Figure 6) shows that the heat exchange between the walls and the ventilation air is limited in the left vertical column. This is because the still high ventilation velocity (hence a large flow rate) does not favor a rapid heat transfer. We note that in the rest of the channel, the fluid is practically isothermal at the same temperature as the walls.

The influence of length on the temperature distribution is shown in Figure IV-31. As the length of the exchanger is increased, there is an increase in the isotherms resulting from the intensification of heat exchange between the walls and the convective jet. The temperature in the air outlet compartment is lower as the length of the exchanger increases. Indeed, the increase of the length generates an increase of the thermal exchange surface between the air and the walls of the exchanger in thermal equilibrium with the ground. The temperature of the ground being lower than that of the ambient air, the air cools down better when the length is greater.

Figure 7 shows the temperature profiles as a function of x in several sections of the exchanger under the influence of the length variation. The analysis of this figure shows that in compartment 1, the temperature profiles as a function of x are identical. This is because in this area the air velocity is higher and the heat exchange is limited. The analysis of the figures in compartments 2 and 3 reveals that the values of the temperature amplitude decrease with the length. Further analysis (Figure 7) of the influence of length shows that there is a threshold length equal to about 40 m from which the increase in length of the exchanger does not significantly influence the temperature of the air at the outlet. According to this result, we consider that the variation of the channel length in the range of 5 m≤L≤40 m is sufficient to obtain a better heat exchange in this type of configuration and consequently a good cooling of the air using the Canadian well.

2.6.3.5. Influence of the Reynolds number

In this section, we examine the effect of the Reynolds number on the structure of the flow, and the thermal field.

2.6.3.6. Structure of the flow

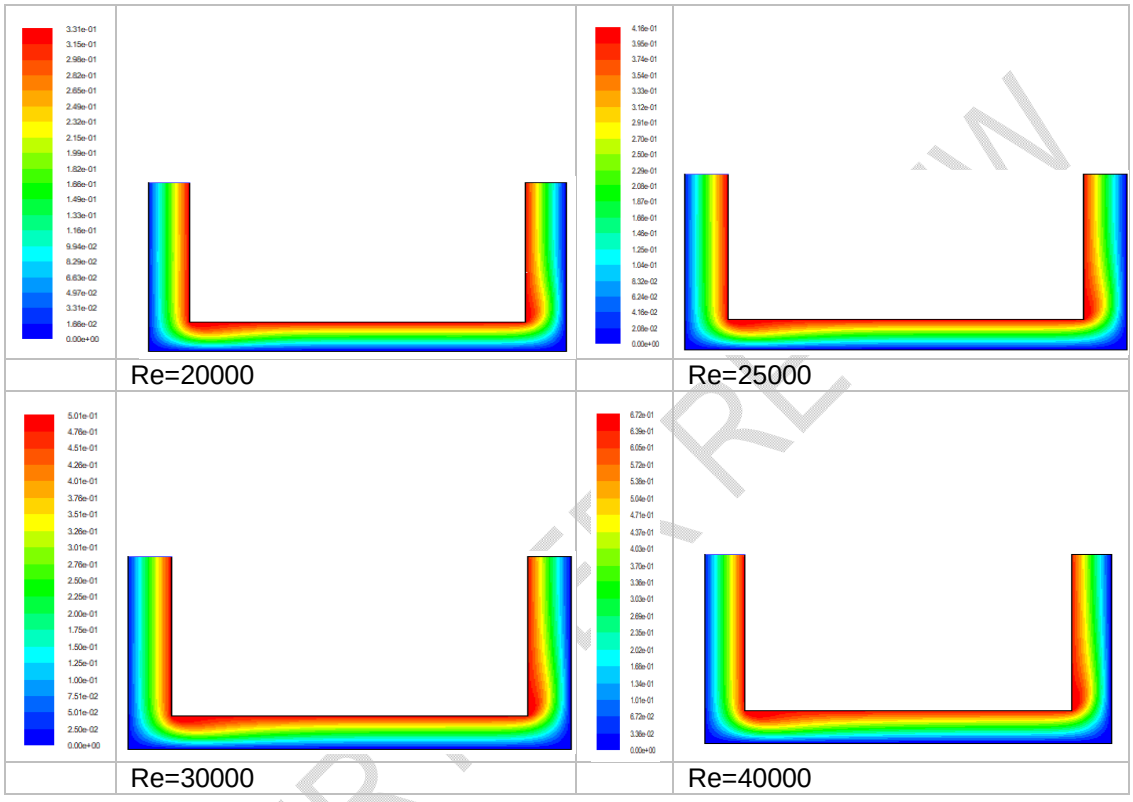

Figure 8: Distribution of streamlines for different Reynolds numbers

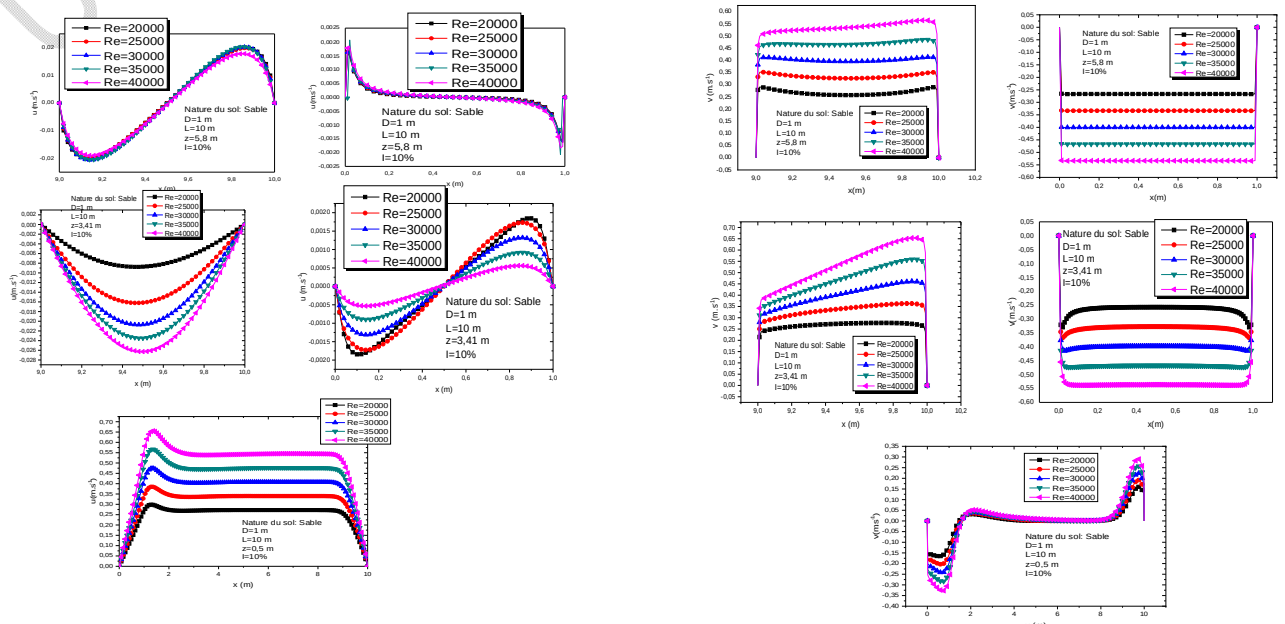

Figure 9: Profile of the u and v components of the velocity under the influence of the Reynolds number

The analysis of Figure 8 showing the distribution of the streamlines for different Reynolds numbers, shows that the structure of the flow has not changed. Figure 9 shows the influence of the Reynolds number on the horizontal (u) and vertical (v) components of the velocity. The u component is dominant in the horizontal part and its amplitude increases with increasing Reynolds number (Figure 9). The increase of the Reynolds number generates an intensification of the forced convection resulting in a vertical component of the velocity which is more and more important in the compartments 1 and 3 where it is dominant. We can also note an increase of the natural convection between the fluid and the walls of the exchanger, but this is not intense enough to significantly modify the structure of the flow.

2.6.3.7. Temperature fields

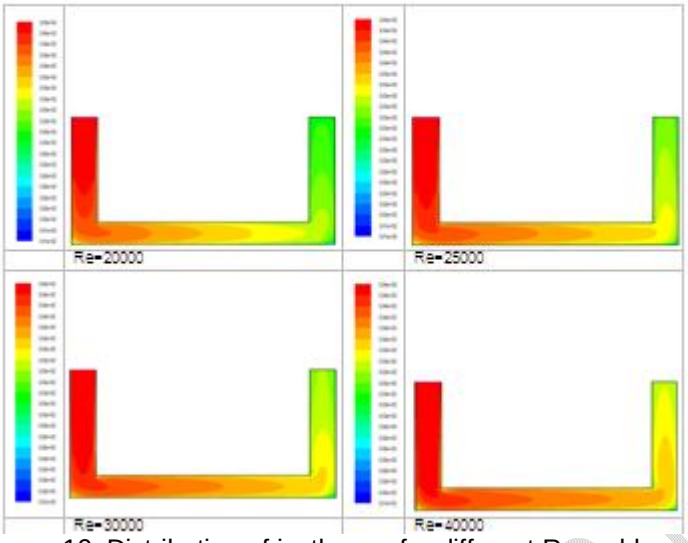

Figure 10: Distribution of isotherms for different Reynolds numbers

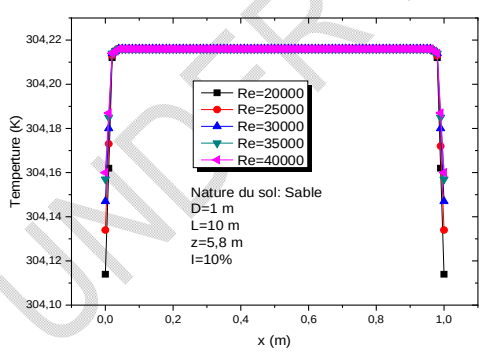

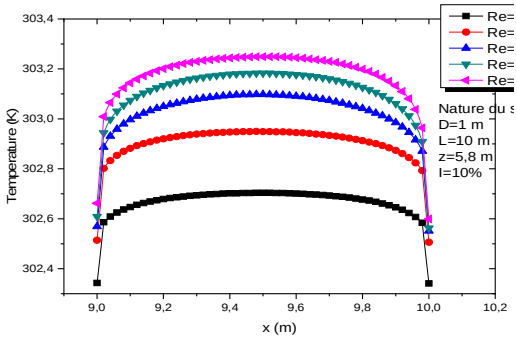

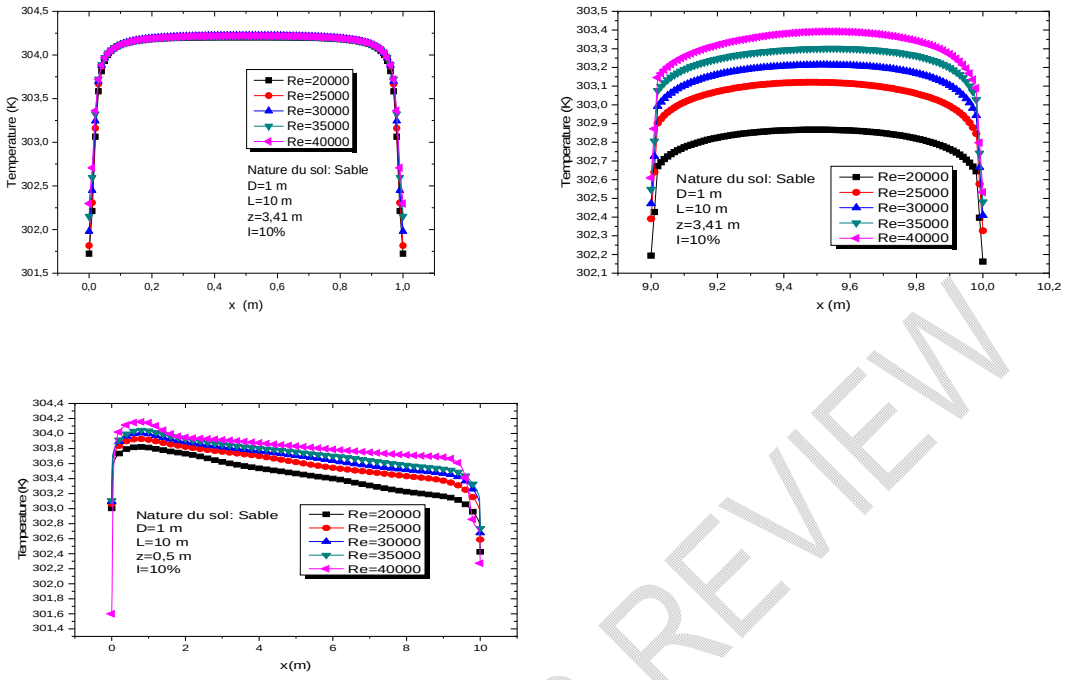

Figure 11: Temperature profile under the influence of the Reynolds number

Figure 10 shows the distribution of isotherms in the exchanger under the influence of the Reynolds number. We observe an increase of the heat transfers in the exchanger with the increase of the Reynolds number marked by the presence of more and more isotherms in the channel. The parabolic isotherms become longer and longer, following the shape of the exchanger. The values of these isotherms increase in the core of the flow as the Reynolds number increases. From these observations, it appears that in order to reduce the air temperature at the exchanger outlet, it is necessary to choose a low Reynolds number but large enough to respect the turbulent flow regime considered in this study. Indeed, the increase of the Reynolds number corresponds to an increase of the inlet velocity and consequently of the air flow at the inlet. The higher the flow rate, the shorter the residence time of the air in the exchanger. This does not favor heat exchange between the air and the walls of the exchanger in thermal equilibrium with the ground. These results are corroborated by the temperature profiles presented in figure 11. This figure shows that the temperature profiles are not affected by the variation of the Reynolds number in compartment 1 due to the very high velocity values which reduce the heat transfer between the air and the vertical walls. In the other compartments, a strong variation of the temperature is observed following the increase of the Reynolds number. The temperature amplitude increases when the Reynolds number and consequently the air flow rate at the inlet increases.

5. Conclusion

This chapter is devoted to the modeling and numerical simulation of the air/ground exchanger in turbulent regime.

The Navier-Stokes dynamic transfer equations and the heat transfer equation have been written taking into account the simplifying assumptions. They were supplemented by spatial-temporal boundary conditions that take into account the climatic conditions of Togo.

The transfer equations and the associated initial and boundary conditions were discretized by the finite volume method solved using the FORTRAN language.

The results were presented in the form of flow structures and temperature fields. Also, we analyzed the influence of the diameter, the length, the air inlet flow through the Reynolds.
The results show that:
- the streamlines are lines open and parallel to each other and to the walls of the exchanger indicating that the various transfers are mainly by forced convection.
- The isotherms are made up of a succession of parabolic shaped cells originating at the inlet of the exchanger and following the shape of the channel.
-The diameter, the length, the Reynolds number, influence to different degrees on the structure of the flow, the distribution of the temperature in the air/soil exchanger.

REFERENCES

S. Thiers, 'Bilans Energétiques et Environnementaux de Bâtiments à Energie Positive', PhD thesis, Ecole Nationale Supérieure des Mines de Paris, November 2008.
M. De Paepe, A. Janssens, "Thermo-hydraulic design of earth-air heat exchangers", Energy and Buildings. vol. 35 (4), 2003, p. 389-397.
V. Badescu, B.Sicre, "Renewable energy for passive house heating: II. Model", Energy and Buildings, vol. 35 (11), 2003, p. 1085-1096.
M. D. Ghosal, G. N. Tiwari, "Modeling and parametric studies for thermal performance of an earth to air heat exchanger integrated with a greenhouse," Energyconversion and management, Vol. 47 (13-14), 2006, pp. 1779-1798.
P.Hollmuller, "Utilisation des échangeurs air-sol pour le chauffage et le rafraîchissement des bâtiments", PhD thesis, University of Geneva, 2002.
Givoni G. "Man, architecture and climate". Paris: Le moniteur, 1978, P.460.
AFNOR NF ISO 9920: "Ergonomics of thermal environments - Determination of thermal insulation and resistance to evaporation of a garment. Paris: AFNOR, 1995, P.54.
ASHRAE, "Chapter 88: Thermal comfort. In: ASHRAE handbook of fundamentals. SI Edition Atlanta: ASHRAE, 1997, P. 8.1-8.28.
B. E. Launder and B. I. Sharma, "Application of the energy-dissipation model of turbulence to the calculation of flow near a spinning disc," Letters in Heat and Mass
Faouzia Benkafada, "Contribution à l'étude de transfert de masse et de chaleur dans un canal poreux", 2008.
S. Zhang, X. Zhao, and S. Bayyuk, "Generalized formulations for the Rhie-Chow interpolation," Journal of Computational Physics, vol. 258, pp. 880 914, Feb. 2014, doi: 10.1016/j.jcp.2013.11.006.
sfer, vol. 1, no. 2, pp. 131-137, Nov. 1974, doi: 10.1016/0094-4548(74)90150-7.
S. Zhang, X. Zhao, and S. Bayyuk, "Generalized formulations for the Rhie-Chow interpolation," Journal of Computational Physics, vol. 258, pp. 880-914, Feb. 2014, doi: 10.1016/j.jcp.2013.11.006.
Versteeg and Malalasekera, An Introduction to Computational Fluid Dynamics..

Nomenclature
cp : Specific heat at constant pressure (J/Kg.K)
i,j : Logical coordinates of the points
λ: Thermal conductivity (w/m.K)
L: Dimensional length of the cavity (m)
x,y
: Coordinates along the horizontal and vertical directions (m)
respectively
u, v : instantaneous horizontal and vertical components of the velocity (m/s)
θ : Temperature (K)
∆θ : Temperature difference (K)
k : turbulent kinetic energy (m^2/s^2)

: turbulent kinetic energy dissipation (m²/ s^3)
p : Pressure (Pa)
g : Gravity (m/s²)
ρ : Density (kg/m^3)
ρ0 : Density at T_0 (kg/m^3)
v : kinematic viscosity (m²/s)
v_t : turbulent kinematic viscosity (m²/s)
μ : dynamic viscosity (Kg/(m.s))
t : time (s)

Dimensionless variables
X,Y :coordinates in the horizontal and vertical directions
U,V :medium horizontal and vertical components of the velocity
T : medium temperature
K : medium turbulent kinetic energy
P : average pressure
: kinematic viscosity
υt: turbulent kinematic viscosity
ε : turbulent kinetic energy dissipation
w : dimensionless verticity
Ψ : dimensionless current function
T_0 : reference temperature
τ : dimensionless time (τ=t V_0/L)
∆t : time step of the simulation
θ : dimensionless temperature ($\theta = \frac{(T-T_f)}{(T_c-T_f)}$)
The constants of the k-ε model
Cμ=0.09; C_1=1.44; C_2=1.92; C_3=0.7; Cθ=0.15; Ck=1.0; Cε=1
Dimensionless numbers
Ri : Richardson number (Ri = Gr/(Re^2))
Gr : Grashof number (Gr = (gβΔTL^3)/v^2)
Re : Reynolds number (Re = UL/v)
Pr : Prandtl number (Pr=υ/α)
Sc : Schmidt number (Sc=μ/ρD)
Greek letters
ϵ : Dimensionless length of the heated part
α : Thermal diffusivity
β=(-1)/ρ_0 ∂ρ/∂T : Coefficient of thermal expansion at pressure
C^te
Indices and Exponents
n : Iteration counter
c : Hot
f : Cold
a: Ambient
e: Exchanger inlet (m^2/s)
t : turbulent (K^(-1))